Supporting Information for

Solid-state nanopore detection of metal ions via DNAzyme and Catalytic Hairpin Assembly

Yesheng Wang, [a, b, e†] Lan Shao, [a, e†] Chunmiao Yu, [a, b, e] Yanru Li, [b, c] Ruiping Wu, [d] Jin Yu, [b, c] Lu Zhou, [f] Tianlu Wang, [f] Yan Zhao, [a, g] Jinbo Zhu [*a, e] and Bingling Li [*b, c]

[a] Y. Wang, L. Shao, C. Yu, Y. Zhao, Prof. J. Zhu
Department of Gastric Surgery, Cancer Hospital of Dalian University of Technology, Shenyang, Liaoning 110042, P. R. China.
E-mail: jinbozhu@dlut.edu.cn

[b] Y. Wang, C. Yu, Y. Li, J. Yu, Prof. B. Li
State Key Laboratory of Electroanalytical Chemistry, Changchun Institute of Applied Chemistry, Chinese Academy of Sciences, Changchun, Jilin, 130022, P.R. China.
E-mail: binglingli@ciac.ac.cn

[c] Y. Li, J. Yu, Prof. B. Li
School of Applied Chemistry and Engineering, University of Science and Technology of China, Hefei, Anhui, 230026, P.R. China.

[d] Dr. R. Wu
Department of Laboratory Medicine, the First Affiliated Hospital of Xi'an Medical University, Xi'an, Shaanxi, 710077, P.R. China.

[e] Y. Wang, L. Shao, C. Yu, Prof. J. Zhu
School of Biomedical Engineering, Faculty of Medicine, Dalian University of Technology, Dalian, Liaoning, 116024, P.R. China

[f] L. Zhou, T. Wang
Department of Radiotherapy, Cancer Hospital of Dalian University of Technology, Shenyang, Liaoning 110042, P. R. China.

[g] Y. Zhao
Provincial Key Laboratory of Interdisciplinary Medical Engineering for Gastrointestinal Carcinoma, Liaoning Cancer Hospital & Institute, Shenyang, Liaoning 110042, P. R. China.

Contents

1. Methods.....Page S3-S5

2. Supporting Figures.....Page S6-S10

Figure S1. Pore size calculation method. .....Page S6

Figure S2. Electrophoresis verification of the GR-5 cleavage reaction and LK-3W-CHA products. .....Page S7

Figure S3. Nanopore characterization results of different Cleavage-CHA reaction products by three nanopores. .....Page S8

Figure S4. Amplitude statistics of nM-level Pb^{2+} cleation-CHA reaction products..Page S9

Figure S5. Cleavage-CHA reaction pathway design for UO_2^{2+} detection and electrophoresis verification.....Page S10

Figure S6. Electrophoresis verification and nanopore results of UO_2^{2+}'s Cleavage-CHA reaction products.....Page S11

3. Supporting Tables.....Page S12

Table S1. Oligonucleotides used in manuscript. .....Page S12

Table S2. Nanopore characterization results analysis of **Fig.S3**.....Page S14

1. Methods

1.1. Materials

Formamide, lithium chloride, sodium chloride, potassium chloride and magnesium chloride are all analytical grade purity and ordered from Sigma-Aldrich (Shanghai) Trading Co., LTD., and all other chemical reagents are analytical grade purity and ordered from Sangon Biotech (China).

All oligonucleotides were ordered from Sangon Biotech (Shanghai, China) and self-PAGE purified. Oligonucleotide sequences are summarized in **Table S1**. If not specified, all oligonucleotides were stored in 1×TNaK (20 mM Tris-HCl, 140 mM NaCl, 5 mM KCl, pH=8.0) or at -20 °C.

1.2. Cleavage reaction and characterization of GR-5

Pb^{2+} induced specific RNA site cleavage reaction of GR-5 DNAzyme was subsequently referred to as cleavage reaction. Before the reaction began, GR-5 was diluted to 2 μM with 1×TNaK solution and annealed: incubated at 65 °C for 3 minutes, then slowly cooled to 37 °C at a rate of 0.1 °C/s before use. Then, 10 μL 2 μM GR-5 was mixed with 10 μL $Pb(NO_3)_2$ solution with appropriate concentration to form a 20 μL cleavage reaction liquid, and were incubated at 37 °C for 1 hour. After the reaction, 7 μL sample was evenly mixed with 2 μL 6 × DNA loading buffer, and 8 μL of the mixture was added to 12% polyacrylamide gel. The PAGE gels were run at a voltage of 350 V under 1×TBE buffer for 90 minutes, then were stained with SYBR GOLD dye for 20 minutes and visualized under UV light.

For the negative controls (water and divalent metal ions control: 250 μM Fe^{2+}, Cu^{2+}, Hg^{2+}, Zn^{2+}, Ca^{2+}), the $Pb(NO_3)_2$ solution in the cleavage reaction were replaced with an equal volume water or a M^{2+} mixed solution of appropriate concentration, and other conditions remain unchanged.

For the actual sample and the actual sample with the added Pb^{2+}, the $Pb(NO_3)_2$ solution in the cleavage reaction were replaced with the corresponding sample of the same volume, and other conditions remain unchanged.

1.3. LK-3W-CHA reactions and Agarose gel characterization

Stock solutions of C1, H1s (H1-A, H1-B and/or H1-C) and H2s (H2-A, H2-B and/or H2-C), H3 were diluted in 1×TNaK to 10 μM. H1s, H2s and H3 were then respectively annealed at 95 °C for 5 min and cooled down to 25 °C at a rate of 0.1 °C/s before use.

To start the LK-3W-CHA reaction, a mixture containing 0.1×C1 (with or without), 1× each necessary H1 (H1-A, H1-B and/or H1-C), 1× each necessary H2 (H2-A, H2-B and/or H2-C), x×H3 (x is equal to the number of H1s or H2s) used were incubated at 25 °C for 3 h. The final buffer condition was that contained 20 mM Tris-HCl (pH=7.5), 140 mM NaCl, 5 mM KCl, 2.5 mM $MgCl_2$ and 500 mM LiCl. To prepare control samples, one or more components might be replaced with respective buffers. The final concentration of C1 is 0 or 50×x nM, each H1 and H2 is 250 nM and H3 is 250×x nM (x is equal to the number of H1s or H2s).

For agarose gel characterization, 7 μL above LK-3W-CHA products were mixed with 2 μL 6×DNA loading buffer, and 8 μL of the mixture were added to 2.5% agarose gels contained 0.08 μL Gel red per mL of gel volume and were prepared by using 1×TAE buffer.

Agarose gels were run at 120 V for 40 min and visualized under UV light.

1.4. Cleavage-CHA Reactions and Agarose gel characterization

After the GR-5 Cleavage reaction completed at 37°C, 6 μL of final product was added to 34 μL LK-3w-CHA liquid to replace C1, and the final concentration of GR-5 is 75 nM, the final volume of Cleavage-CHA reaction is 40 μL. The LK-3w-CHA liquid included 2 μL 5 μM H1-A/B/C, 2 μL 5 μM H2-A/B/C, 6 μL 5 μM H3, 2 μL 10M LiCl, 2 μL 50 mM $MgCl_2$, and 12 μL 1×TNaK to form a 34 μL mixed solution. The Cleavage-CHA reaction was kept at 25 °C for 3 hours, the products were characterized by 2.5% agarose gel electrophoresis under the same conditions as in **1.3.**

1.5. Nanopore detection of LK-3W-CHA and Cleavage-CHA Reaction products

All nanopore data collections were carried out on the nanopore test platform designed and built by our laboratory. Before nanopore measurement, 20 μL LK-3W-CHA or Cleavage-CHA Reaction products, 10 μL formamide and 20 μL 10M LiCl were mixed together to form a 50 μL sample liquid, and 1×TNaK, formamide and 10M LiCl were mixed with a ratio of 2:1:2 to form a nanopore buffer. The sample liquid was injected into the glass sample pool (cis-end) outside the nanopore tip, and the nanopore buffer with the same ionic strength as the sample liquid in the sample pool (4M LiCl, 20% formamide by volume fraction, and the remaining part was filled with the same buffer solution as the sample system) was injected into the glass nanopore (trans-end). The bubbles in the pores are expelled to ensure that the electrolyte solution is fully injected into the nanopore tip.

Glass nanopores were generated on a laser-heated pipette puller (P-2000, Sutter Instrument) by pulling quartz capillaries (outer diameter 1.0 mm and inner diameter 0.7 mm, Sutter Instrument), the program parameter is: HEAT=760, FIL=4, VEL=29, DEL=140, PUL=170. Two chlorinated silver electrodes were placed at the two sides of the nanopore and connected to an Axon Axopatch 200B amplifier (Molecular Devices), which applied a voltage (600 mV) to drive the DNA through nanopores and recorded the current signal. The signal was filtered with a lowpass Bassel filter of 5 kHz and digitized with a DigiData 1550B digitizer (Molecular Devices) at a sample rate of 250 kHz. The current signal was processed using Clampfit 11.2 software (Molecular Devices) and MATLAB-based software, and the current traces were gained from origin data by using Clampfit 10.6. All the nanopore experiments were at the room temperate (25°C)

1.6. Cleavage reaction and characterization of UO_2^{2+}-responsive DNAzyme

UO_2^{2+} induced specific RNA site cleavage reaction of DNAzyme was subsequently referred to as cleavage reaction. U-DNAzyme was diluted in water to 10 μM as the storge solution, and it was diluted to 2 μM with MES buffer (10 mM MES, 300 mM NaCl, pH=5.5) and annealed: incubated at 65 °C for 3 minutes, then slowly cooled to 25 °C at a rate of 0.1 °C/s before use. Then, 10 μL 2 μM U-DNAzyme was mixed with 10 μL $UO_2(NO_3)_2$ solution with appropriate concentration to form a 20 μL cleavage reaction liquid, and were incubated at 25 °C for 30 min. After the reaction, 7 μL sample was evenly mixed with 2 μL 6×DNA loading buffer, and 8 μL of the mixture was added to 12% polyacrylamide gel. The PAGE gels were run at a voltage of 350 V under 1×TBE buffer for 90 minutes, then were stained with SYBR GOLD dye for 20 minutes and visualized under UV light.

1.7. Gel characterization of Openlink and HpC1's combination

Openlink and HpC1 were diluted in water to 10 μM as the storge solution, and diluted

to 2 μM in 1×TNaK then annealed: incubated at 95 °C for 5 minutes, then slowly cooled to 25 °C at a rate of 0.1 °C/s before use. The whole reaction liquid included 0 or 1 μL 2 μM Openlink, 0 or 1 μL 2 μM HpC1, and added 1×TNaK to form a 10 μL mixed solution. The hybridization was carried out at 25 °C for 1 hour. After the reaction, 7 μL sample was evenly mixed with 2 μL 6×DNA loading buffer, and 8 μL of the mixture was added to 12% polyacrylamide gel. The PAGE gels were run at a voltage of 350 V under 1×TBE buffer for 90 minutes, then were stained with SYBR GOLD dye for 20 minutes and visualized under UV light.

1.8. UO_2^{2+}'s Cleavage-CHA Reactions and Agarose gel characterization

After the U-DNAzyme Cleavage reaction completed at 25°C , 3 μL of final product was mixed with 3 μL 1 μM HpC1, and carried out at 25 °C for 1 hour, then they were added to 34 μL LK-3w-CHA liquid to replace C1, and the final concentration of U-DNAzyme and HpC1 is 150 nM, the final volume of Cleavage-CHA reaction is 40 μL. The LK-3w-CHA liquid included 2 μL 5 μM U-H1-A/B/C, 2 μL 5 μM U-H2-A/B/C, 6 μL 5 μM U-H3, 2 μL 10M LiCl, 2 μL 50 mM $MgCl_2$, and 12 μL 1×TNaK to form a 34 μL mixed solution. The Cleavage-CHA reaction was kept at 25°C for 3 hours, the products were characterized by 2.5% agarose gel electrophoresis under the same conditions as in **1.3.**

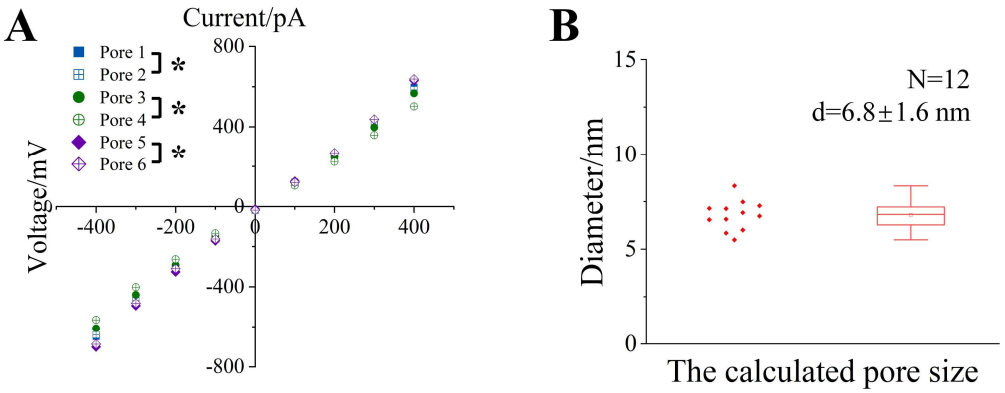

Figure S1. Pore size calculation method. (A) I-V characteristics of conical glass nanopores in 0.1M KCl (N=6). (B) Calculated nanopore diameters from 12 pores. Notes: Symmetrical nanopores fabricated from one capillary were denoted by an asterisk.

we could use the electrochemical measurement and estimate the nanopore diameter according to the classical Equation (S1). [1-3] For example, we chose the current data between -100 mV and 100 mV because in this interval the linear and rectification ratio is close to 0. It is speculated that this slight deviation is due to the shape change of the nanopore tip region caused by high energy electron radiation.

$$a = \frac{1}{\pi \kappa R \mathrm{ta}\ \frac{\theta}{2}} \qquad \text{(S1)}$$

Where R is the measured pipette resistance, κ is the specific resistance of the electrolyte used (κ=1.2 S/m in 0.1M KCl), θ is the cone angle (θ=12°) and a is the radius of the nanopore at the tip of the nanopipette.

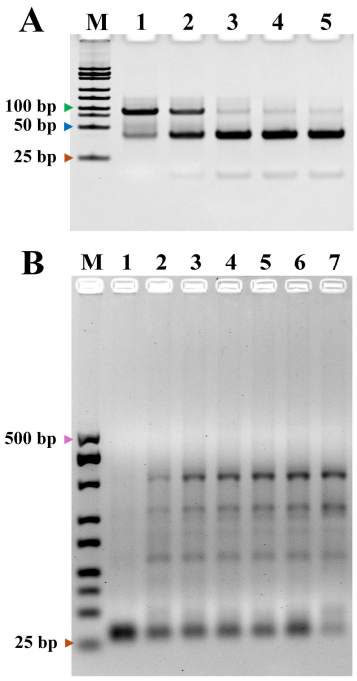

Figure S2. Electrophoresis verification of the GR-5 cleavage reaction and LK-3W-CHA products. (A) 12% Polyacrylamide gel electrophoresis that proves the cleavage reaction is efficient. The lane 1-5 is 1 μM GR-5 with 0/5/50/500/5000 nM Pb^{2+}. (B) 2.5% Agarose gel electrophoresis of Cleavage-CHA reaction products at different conditions. All the groups (1-7) have the needed hairpin substrates for Y3. The differences between them lie in C1 (or the component used to replace C1). Lane 1 is blank (without C1) and lane 7 is with C1. Cleavage reaction products were added in lane 2-6, which correspond to lane 1-5 in **Fig. S2A**.

We further investigated the efficiency of the cleavage reaction and the CHA reaction under lower lead concentrations. As shown in **Fig. S2A**, the cleavage reaction could still be observed at a Pb^{2+} concentration as low as 5 nM (lane 2), with the corresponding reaction products detectable via PAGE. The extent of the cleavage reaction varied significantly under different Pb^{2+} concentrations, which in turn affected the efficiency of the subsequent CHA reaction. The Agarose gel electrophoresis results in **Fig. S2B** demonstrate that the CHA reaction efficiency increased correspondingly with higher Pb^{2+} concentrations. These results indicate that our designed cleavage-CHA reaction system exhibits a favorable concentration-dependent response to low levels of Pb^{2+}.

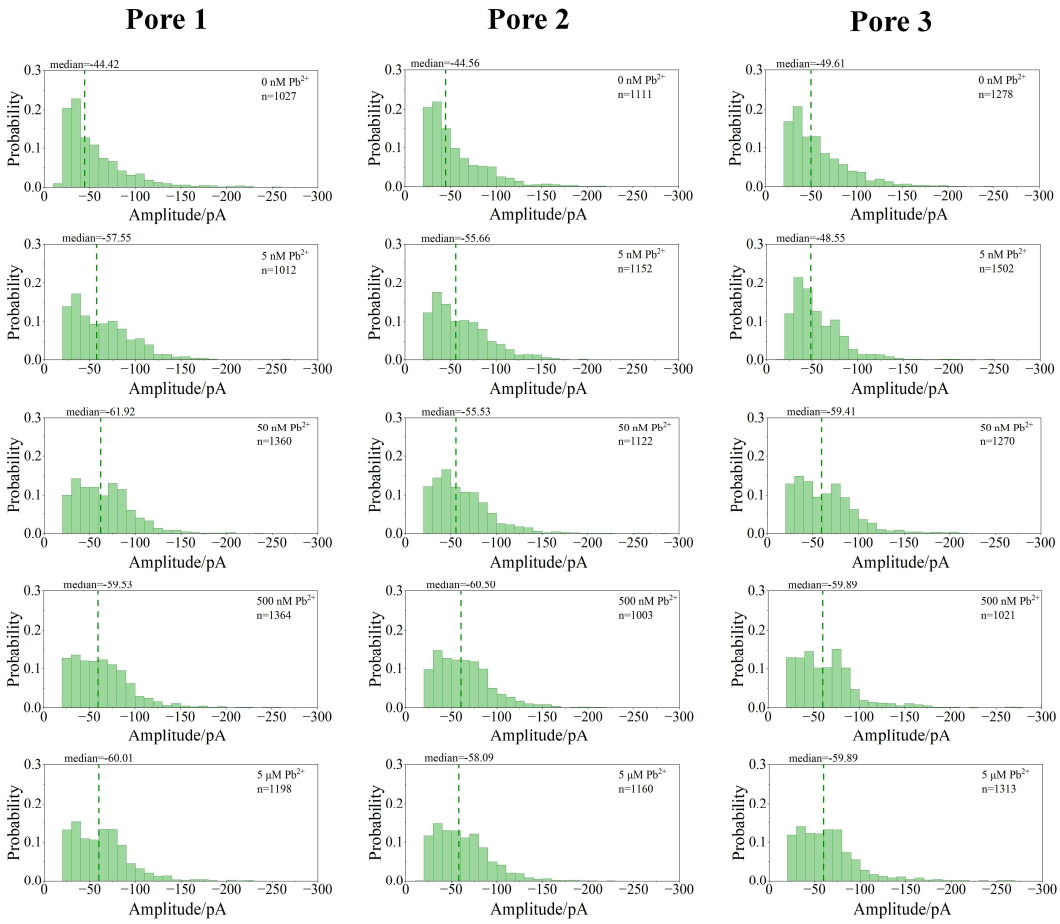

Figure S3. Nanopore characterization results of different Cleavage-CHA reaction products by three nanopores. The Cleavage-CHA reaction products corresponding respectively 0/5/50/500/5000 nM Pb^{2+} (**Fig. S2B**, lane 2-6) and the data in each column were collected by the same nanopore (labeled Pore 1, Pore 2, Pore 3).

We characterized the cleavage-CHA reaction products under low Pb^{2+} concentrations using three distinct nanopores and performed statistical analysis of the Amplitude, as shown in **Fig. S3** (more detailed statistics are provided in **Table S2**). Both the median and mean values of the translocation current showed an increasing trend with higher Pb^{2+} concentrations. These results demonstrate that by comparing the nanopore event statistics between the background (GR-5 only) and post-reaction samples, we can make a qualitative estimation of the Pb^{2+} content in the test samples.

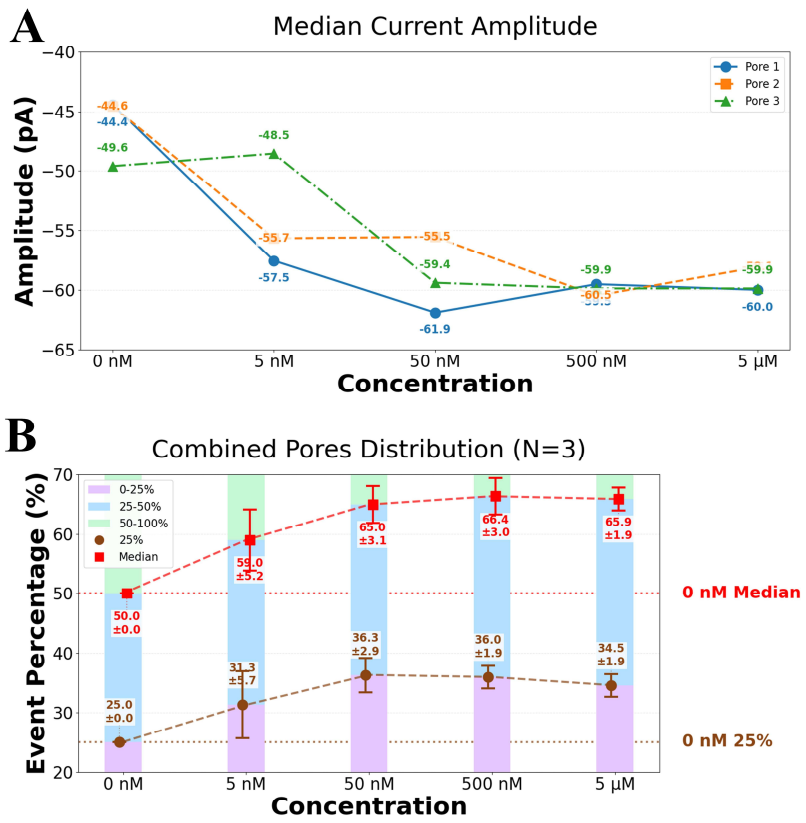

Figure S4. Amplitude statistics of nM-level Pb^{2+} Cleavage-CHA reaction products. (A) The median of amplitude of Cleavage-CHA reaction products corresponding to each concentration from Pore 1-3. (B) The median and 25% position amplitude corresponding to 0 nM Pb^{2+}(Background) compared to other concentrations (data from **Table S2**).

From **Fig. S4A**, we observe the median of ranslocation currents of the cleavage-CHA reaction products show significant increases in the presence of Pb^{2+} compared to the no-Pb^{2+} control group. This phenomenon demonstrates good reproducibility across different nanopore experiments.

Further statistical analysis using the no-Pb^{2+} control group as reference (with the 25% position and median current values as benchmarks) reveals that Pb^{2+}'s exist leads to a marked increase in the proportion of events with currents below the control median (blue and purple portions) (**Fig. S4B**), with a similar trend observed for the 25% position threshold. These findings indicate that Pb^{2+} facilitates the formation of larger nucleic acid assemblies, thereby confirming successful transduction of Pb^{2+} to Y3 molecules.

While quantitative concentration determination remains challenging, our method demonstrates reliable detection of Pb^{2+} at concentrations as low as 5 nM.

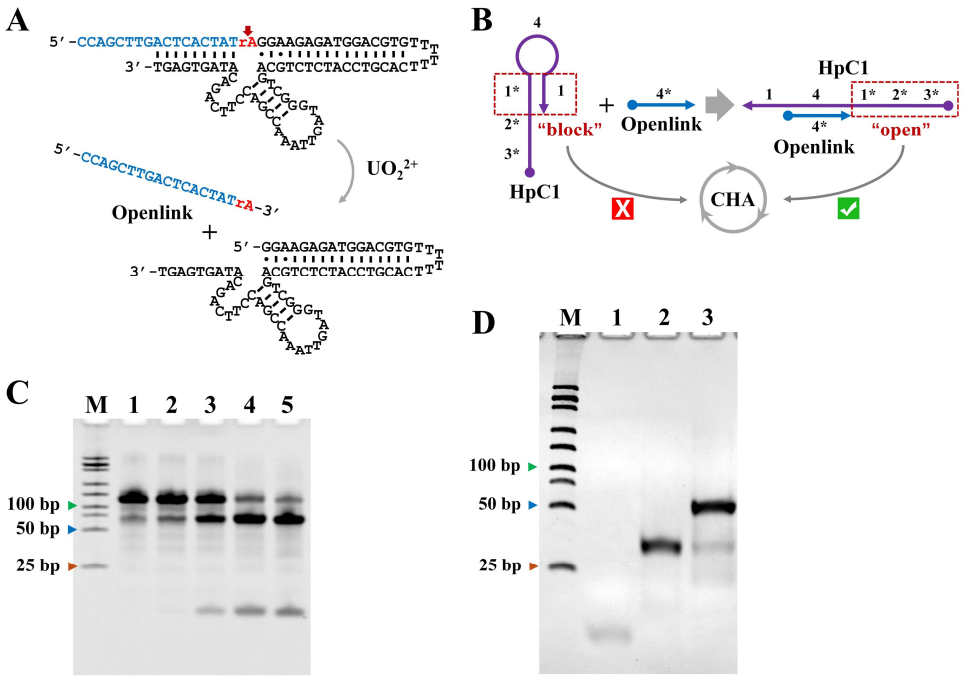

Figure S5. Cleavage-CHA reaction pathway design for UO_2^{2+} detection and the electrophoresis verification. (A) Schematic of cleavage reaction activated by UO_2^{2+}. (2) The newly introduced transduction. The cleavage chain "Openlink" opening the hairpin structure HpC1 at the "blocked" state through hybridization, and converting it into the "open" state, releasing the domain "1*" to catalyze the CHA reaction. (C) 12% Polyacrylamide gel electrophoresis that proves the cleavage reaction is efficient. The lane 1-5 is 1 μM U-DNAzyme with 0/10/100/1000/10000 nM UO_2^{2+}. (D) 12% Polyacrylamide gel electrophoresis that proves the combine of Openlink and HpC1 is efficient. Lane 1 is Openlink, lane 2 is HpC1 and lane 3 is the hybrid products of Openlink and HpC1 under the same concentration.

To validate the versatility and scalability of our approach, we incorporated a transduction component into the cleavage-CHA reaction system, to avoid extra design for CHA pathway. As shown in **Fig. S5A**, we engineered a UO_2^{2+}-responsive DNAzyme by extending its 5' terminus with approximately 8 nucleotides, enabling the cleavage reaction to release a 17-nt oligonucleotide fragment (named as "Openlink"). The transduction mechanism, illustrated in **Fig. S5B**, demonstrates that Openlink can hybridize with a hairpin DNA structure (HpC1) containing the embedded CHA initiator sequence C1. This hybridization event triggers the release of a locked structural domain ("1*"), thereby enabling the resulting assembly to function as an effective C1 catalyst for the CHA reaction. We characterized the modified cleavage-CHA reaction process using electrophoretic analysis. Our results show that the cleavage reaction remains detectable at UO_2^{2+} concentrations as low as 10 nM (**Fig. S5C**, lane 2) while the concentration of U-DNAzyme was 1 μM, with corresponding reaction products clearly visible via PAGE. Furthermore, the Openlink (**Fig. S5D**, lane 1) and HpC1 (**Fig. S5D**, lane 2) were incubated under the same concentration at 25°C for 1 hour. The resulting products (**Fig. S5D**, lane 3) exhibited high hybridization efficiency, as evidenced by distinct electrophoretic banding patterns.

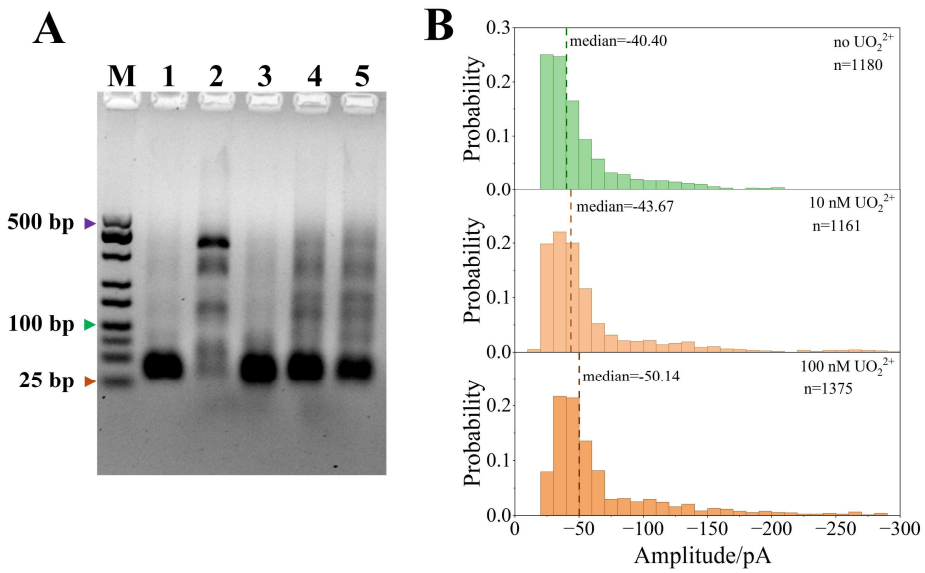

Figure S6. Electrophoresis verification and nanopore results of UO_2^{2+}'s Cleavage-CHA reaction products. (A) 2.5% Agarose gel electrophoresis of UO_2^{2+}'s Cleavage-CHA reaction products. Hairpin substrates for Y3 were added in all groups (1-5). The differences between them lie in C1 (or the component used to replace C1). Lane 1 is blank (without C1) and lane 2 is with C1. Cleavage reaction products were added in lane 3-5 (0/10/100 nM UO_2^{2+}), which correspond to lane 1-3 in **Fig. S5C**. (B) Histograms of amplitude of 0/10/100 nM UO_2^{2+}.

As shown in **Fig. S6A**, significant differences were observed under various reaction conditions: when the reaction system contained neither C1 nor U-DNAzyme (lane 1), or contained only U-DNAzyme with HpC1 (lane 3), almost no reaction was detected. In contrast, the reaction showed high completion efficiency in the presence of C1 (lane 2). Notably, in cleavage reaction systems containing either 10 nM (lane 4) or 100 nM (lane 5) UO_2^{2+}, distinct bands corresponding to CHA assemblies were clearly observed. Furthermore, by comparing the remaining substrate levels, it was evident that the reaction completion under 100 nM UO_2^{2+} conditions was significantly higher than that under 10 nM conditions. We characterized UO_2^{2+}'s cleavage-CHA reaction products corresponding to lanes 3, 4, and 5 in **Fig. S6A** with one same nanopore and generated statistical histograms based on their translocation current (Amplitude) signals (**Fig. S6B**). The experimental results demonstrated that compared to the background control (**Fig. S6A**, lane 3), both the 10 nM (**Fig. S6A**, lane 4) and 100 nM UO_2^{2+} (**Fig. S6A**, lane 5) reaction systems showed increased median Amplitude values. Specifically, the mean Amplitude improved from -53.81 pA in the background group to -63.61 pA in the 10 nM UO_2^{2+} group, and further increased to -75.94 pA under 100 nM UO_2^{2+} conditions. These findings not only confirm the effectiveness of our method for UO_2^{2+} detection but also indicate that our designed approach holds potential for extension to other metal ion detection applications, maintaining reliable qualitative analysis even at concentrations as low as 10 nM.

Table S1. Oligonucleotides used in manuscript. All sequences were purified with high-pressure liquid chromatography and then self-PAGE purified.

Sequences of Oligonucleotides.		
Name	**Sequence 5'-3'**	**Notes**
Sequences of Pb^{2+}'s cleavage-CHA reaction		
GR-5 (DNAzyme)	[3*|2*|1*|rA|……|1|G}	rA present RNA site
	[CGACATCT|AACCTAGC|TCACTAT|rA|GGAAGAGATGATGTCTGTTTTTTTACAGACATCATCTCTGAAGTAGCGCCGCCGT|ATAGTGAG}	
C1	[3*|2*|1*}	
	[CGACATCT|AACCTAGC|TCACTAT}	
H1-A	[TG|1|2|3|T|4|5|3*|2*}	
	[TG|GATAGTGA|GCTAGGTT|AGATGTCG|T|GAGAGAAC|GTGATGAA|CGACATCT|AACCTAGC}	
H1-B	[TG|1|2|3|T|4|6|3*|2*|5*-}	"5*-" means 2 bases shorter than the origin domain "5*"
	[TG|GATAGTGA|GCTAGGTT|AGATGTCG|T|GAGAGAAC|GTGCATGAT|CGACATCT|AACCTAGC|TTCATC}	
H1-C	[TG|1|2|3|T|4|7|3*|2*}	
	[TG|GATAGTGA|GCTAGGTT|AGATGTCG|T|GAGAGAAC|CCGATATG|CGACATCT|AACCTAGC}	
H2-A	[GGTT|3|5*|4*|1*|7|4|5*|2}	
	[GGTT|AGATGTCG|TTCATCAC|GTTCTCTC|TCACTATC|CTTGTCTC|GAGAGAAC|GTGATGAA|GCTAGGTT}	
H2-B	[3|6*|4*|1*|7|4|6|9*-}	"9*-" means 1 base shorter than the origin domain "9*"
	[AGATGTCG|ATCATGCAC|GTTCTCTC|TCACTATC|CTTGTCTC|GAGAGAAC|GTGCATGAT|CATATCG}	
H2-C	[3|9*|4*|1*|7|4|9|6*-}	"6*-" means 1 base shorter than the origin domain "6*"
	[AGATGTCG|CATATCGG|GTTCTCTC|TCACTATC|CTTGTCTC|GAGAGAAC|CCGATATG|ATCATGCA}	
H3	[4*|7*|1|T|3*|2*|1*|7|CA}	
	[GTTCTCTC|GAGACAAG|GATAGTGA|T|CGACATCT|AACCTAGC|TCACTATC|CTTGTCTC|CA}	
Sequences of UO_2^{2+}'s cleavage-CHA reaction		
U-DNAzyme	[CCAGCTTGACTCACTAT|rA|GGAAGAGATGGACGTGTTTTTTCACGTCCATCTCTGCAGTCGGGTAGTTAAACCGACCTTCAGACATAGTGAGT}	rA present RNA site
Openlink	[4*}	
	[CCAGCTTGACTCACTAT}	
HpC1	[3*|2*|1*|4-|1|G}	The end of domain 4-delete a base "G"
	[CGACATCT|AACCTAGC|TCACTGAC|ATAGTGAGTCAAGCTG|GTCAGTGA|G}	

C1	[3*|2*|1*}	
	[CGACATCT|AACCTAGC|TCACTGAC}	
U-H1-A	[TG|1|2|3|T|4|5|3*|2*}	
	[TG|GTCAGTGA|GCTAGGTT|AGATGTCG|T|GAGAGAAC|GTGATGAA|CGACATCT|AACCTAGC}	
U-H1-B	[TG|1|2|3|T|4|6|3*|2*|5*-}	"5*-" means 2 bases shorter than the origin domain "5*"
	[TG|GTCAGTGA|GCTAGGTT|AGATGTCG|T|GAGAGAAC|GTGCATGAT|CGACATCT|AACCTAGC|TTCATC}	
U-H1-C	[TG|1|2|3|T|4|7|3*|2*|8-}	"8-" means 2 bases shorter than the origin domain "8"
	[TG|GTCAGTGA|GCTAGGTT|AGATGTCG|T|GAGAGAAC|CCGATATG|CGACATCT|AACCTAGC|CTATCC}	
U-H2-A	[2-|3|5*|4*|1*|9|4|5|2}	"2-" means 4 bases shorter than the origin domain "2"
	[GGTT|AGATGTCG|TTCATCAC|GTTCTCTC|TCACTGAC|CTTGTCTC|GAGAGAAC|GTGATGAA|GCTAGGTT}	
U-H2-B	[3|6*|4*|1*|9|4|6|7*-}	"7*-" means 1 base shorter than the origin domain "7*"
	[AGATGTCG|ATCATGCAC|GTTCTCTC|TCACTGAC|CTTGTCTC|GAGAGAAC|GTGCATGAT|CATATCG}	
U-H2-C	[3|7*|4*|1*|9|4|7|6*-}	"6*-" means 1 base shorter than the origin domain "6*"
	[AGATGTCG|CATATCGG|GTTCTCTC|TCACTGAC|CTTGTCTC|GAGAGAAC|CCGATATG|ATCATGCA}	
U-H3	[4*|9*|1|T|3*|2*|1*|9|CA}	
	[GTTCTCTC|GAGACAAG|GTCAGTGA|T|CGACATCT|AACCTAGC|TCACTGAC|CTTGTCTC|CA}	

Table S2. Nanopore characterization results analysis of **Fig.S3**

Nanopore	Concentration	Number of Events	Avg. Amplitude (pA)	25% Position (pA)	Median (pA)	75% Position (pA)	Below 0 nM's 25% Position	Below 0 nM's Median
Pore 1	**0 nM**	1027	-56.19	-69.94	-44.42	-31.10	-	-
	5 nM	1012	-63.98	-84.44	-57.55	-35.91	392 / 38.74%	650 / 64.23%
	50 nM	1360	-65.66	-83.22	-61.92	-40.64	573 / 42.13%	949 / 69.78%
	500 nM	1364	-64.29	-81.11	-59.53	-39.19	511 / 37.46%	942 / 69.06%
	5 µM	1198	-62.88	-79.24	-60.01	-37.45	440 / 36.73%	794 / 66.28%
Pore 2	**0 nM**	1111	-55.84	-70.46	-44.56	-31.26	-	-
	5 nM	1152	-62.28	-80.86	-55.66	-36.76	402 / 34.90%	739 / 64.15%
	50 nM	1122	-63.40	-77.46	-55.54	-38.83	376 / 33.51%	739 / 65.86%
	500 nM	1003	-65.00	-80.96	-60.50	-40.20	383 / 38.19%	699 / 69.69%
	5 µM	1160	-63.11	-79.37	-58.09	-38.86	420 / 36.21%	801 / 69.05%
Pore 3	**0 nM**	1278	-58.77	-74.59	-49.61	-33.51	-	-
	5 nM	1502	-56.15	-70.96	-48.55	-35.76	303 / 20.17%	730 / 48.60%
	50 nM	1270	-63.66	-81.53	-59.41	-37.82	423 / 33.31%	753 / 59.29%
	500 nM	1021	-63.96	-79.27	-59.89	-39.43	329 / 32.22%	616 / 60.33%
	5 µM	1313	-65.02	-78.79	-59.89	-39.59	403 / 30.69%	819 / 62.38%

Reference

[1] Z. T. Zhu, X. Z. Duan, Q. Li, R. P. Wu, Y. S. Wang, B. L. Li, *J. Am. Chem. Soc.* **2020**, *142*, 9, 4481–4492.

[2] Z. T. Zhu, R. P. Wu, B. L. Li, *Chem. Sci.* **2019**, *10*, 1953-1961.

[3] Y. Fu, H. Tokuhisa, L. A. Baker, *Chem. Commun.*, **2009**, *32*, 4877-4879.